ACTA SCIENTIFIC AGRICULTURE (ISSN: 2581-365X)

Volume 3 Issue 6 June 2019

Review Article

Grasps of Robot Manipulator When Overloading Solid High-Radioactive Elements and their Calculation

Kaimov S[1], Kostopoulos G[4], Kaimov A[1], Pichugin A[5], Kaimov Ab[1], Kaiym T[2]* and Kaimova G[3]

[1]*Kazakh National University, Almaty, Republic of Kazakhstan*

[2]*Almaty University of Power Engineering and Telecommunications (AUPET), Almaty, Republic of Kazakhstan*

[3]*Kazakh Academy of Transport and Communications Named After M. Tynyshpaev, Republic of Kazakhstan*

[4] *University of Maryland University, USA*

[5]*Department of Mathematics, Brunel University, UK*

***Corresponding Author:** Kaiym T, Almaty University of Power Engineering and Telecommunications (AUPET), Almaty, Republic of Kazakhstan.

Received: March 12, 2019; **Published:** May 10, 2019

DOI: 10.31080/ASAG.2019.03.0474

Abstract

In this paper considers the problem of simulating two grasping schemes of the robot manipulator, created by the authors for the overload of solid highly radioactive waste of fuel elements. Two schemes, previously proposed by the authors as grasps, are investigated. One - rod, the second - innovative with flexible actuators. For the grasps considered, some results are given: static calculations for flat grasping models; 3D models of grasp; the strength and rigidity of one 3D model are calculated.

Keywords: Gripper; Strength; Rigidity; Schema; Model

Introduction

In this paper, the authors develop the calculation of two schemes of grasps of a robot manipulator for reloading solid highly radioactive waste of fuel elements. It is based on known approaches to this problem [1,2]. Here, for the first scheme, a gripper with pneumatic drive is considered, for the second scheme flexible traction elements are used.

Below is given the kinematic scheme of the first grasp and its 3D model, which is calculated for strength and rigidity. This scheme had developed based on the recommendations of the work [3].

The relationship between the force on the drive and the clamping force of the workpiece (Figure 1a) is determined from the static equilibrium conditions:

a 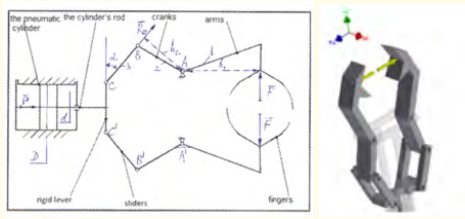 b

Figure 1: scheme of the mechanism and 3D model of grasping by [3].

From the condition of equilibrium of forces $\sum F_i = 0$ at point C for the upper symmetric branch C-B-A, we have:

$$-\frac{P}{2} + R_{23}\sin\alpha = 0 \text{ or } R_{23} = \frac{P}{2\sin\alpha} = 0 \quad (1)$$

From the condition of equilibrium of the moments of forces $\sum M_{A_i} = 0$ relative to the point A for the upper symmetric branch C-B-A, we have:

$$Fh_1 - R_{23}h_2 = 0 \text{ or } P = 2\frac{Fh_1}{h_2}\sin\alpha \quad (2)$$

Here-1 and 2 constitute one rigid link; R_{23}–reaction in the hinge B; α - angle between stem and link 3 in hinge C; h_1, h_2– shoulders of moments of forces F, R_{23}.

The calculation of the 3D model (Figure 1b) of the seizure, developed by the authors in [3]. The load on the teeth of the grasp is taken to be 400 N, the simulation was carried out on "Autodesk Inventor" [4]. Patterns of distribution of stresses, displacements, factors of safety factor, deformations, contact pressures are obtained. Figure 2 shows the distribution of reduced stresses according to Mises. On the left, there is a color scale with stress values. Voltages are given in the figure in megapascals (MPa), the maximum being 784.2 MPa and it appears in the vicinity of the model point corresponding to point A of the gripper circuit (Figure 1a).

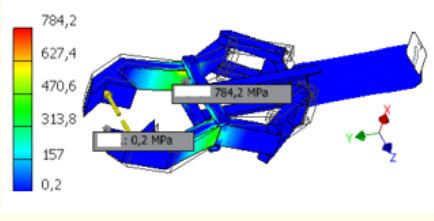

Figure 2: Calculation of the 3D model for strength.

Figure 3 shows the patterns of elastic displacements of the gripper characterizing its positioning accuracy due to the rigidity of the structure. On the left, there is a color scale with the values of elastic displacements. Elastic displacements are given in the figure in millimeters. As can be seen from the distribution pattern, the largest elastic displacements are located in the region of the grasp teeth. For this model, the maximum displacement is located at the tip of the teeth and is 0.8839 mm.

Figure 4 shows the distribution pattern of the safety factor, showing how many times the tensile strength exceeds the reduced Mises stresses at the points of the model. On the left in the figure is a color scale with the values of safety factors. The safety factor is a dimensionless quantity. The values of the safety factor indicate the weakness of the design in the vicinity of link 1.

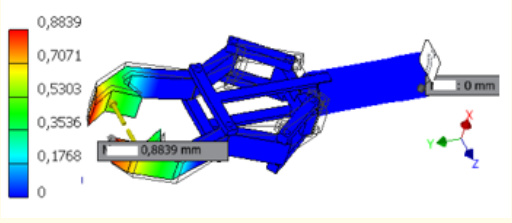

Figure 3: Calculation of the 3D model for rigidity.

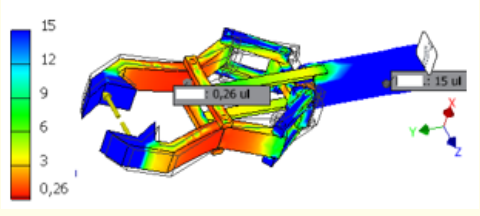

Figure 4: 3D model calculation for safety factor.

Below we study three- phalanges adaptive gripper of the robot manipulator for transferring the fuel element from the intermediate container to the main container for solid radioactive waste when it is buried in the repository (cemetery) of solid highly radioactive waste. An approximate model of such a grasp was proposed by the authors in [5] (Figure 5).

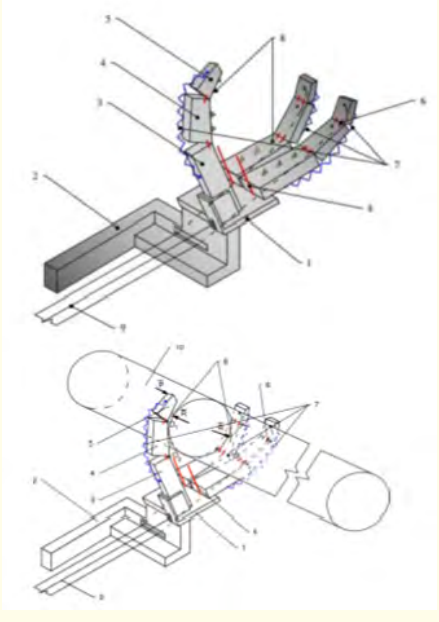

Figure 5

Three- phalanges adaptive gripper of the robot manipulator for transferring the fuel element from the intermediate container to the main container for solid radioactive waste when it is buried in the repository (cemetery) of solid highly radioactive waste: 1-tile-base for fixing the main phalanx of the lever; 2-mounting arm of the manipulator; 3-basic phalanx; 4-middle phalanx; 5-terminal phalanx; 6-hinge fixing adjacent phalanges with each other; 7-tightening spring; 8-holding tooth; 9-flexible traction element, 10 - fuel element.

In this work further researches of this grasp are continued:

- Its flat model is developed (Figure 6). For it has received, the relations connecting the metric and force parameters of the model are obtained;
- The 3D model is developed (Figure 7). This scheme was developed taking into account the recommendations of [5-7].

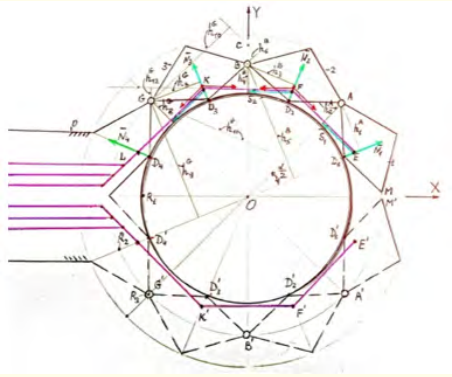

Figure 6: Flat gripper scheme with flexible drives.

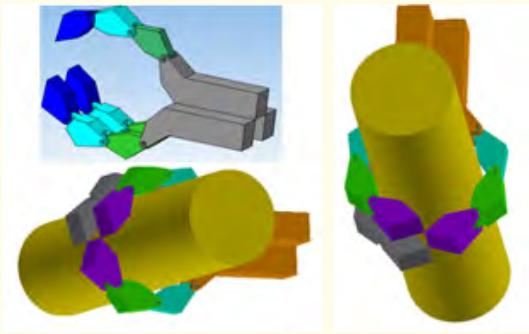

Figure 7: 3D model of grasping with flexible connections.

Consider a flat gripper model with flexible drives (Figure 6). The radius R_1 of fuel element is in the grip (Figure 5-7). And the opposite end of the first flexible traction element passes through the point L on the base tile. And then the flexible traction element goes to the drive. The end of the second flexible traction element is fixed at point F of the middle phalanx. The second flexible traction element then passes through the opening K of the main phalanx. And the opposite end of the flexible traction element passes through the point L on the base tile. And then the second flexible traction element goes to the drive. The end of the third flexible traction element is fixed at the point K of the main phalanx. And the opposite end of it passes through the point L on the tile-base. And then the third flexible traction element goes to the drive.

The main stages of calculation

The phalanges are quadrangles symmetrical with respect to the radial line (Figure 6). The upper points of these quadrilaterals lie on a radial line, at a distance R3 from the point O. The hinges G, B and A are located on a circle of radius R2. The arcs $\breve{GB}, \breve{BA}, \breve{AM}$ are based on the central angles . Radius of circles are related by the relation: $R_3 > R_2 > R_1$ grasp teeth are located at points D_1, D_2, D_3, D_4 the upper symmetrical branch of the G-B-A-M gripper. And in points D'_1, D'_2, D'_3, D_4 the lower symmetrical branch of the G'-B'-A'-M 'grip. The points E, F, K, and L are located at a distance "a" in the radial direction from the teeth D_1, D_2, D_3, D_4. Moreover, the distance "a" is such that $0<a<(R_2 - R_1)$. Then the flexible traction element creates moments of force to hold the fuel element in the gripper. From the condition of non-tangency, the flexible traction element to the circumference of the part has $(R_1 + a)\cos(\alpha/2) > R_1$ or $a > R_1/\cos(\alpha/2) - R_1$, where α – the central angle (Figure 6). Let then the coverage of the fuel element by the three phalanges of the finger was sufficient for a semicircle. Let's find the internal effort $\bar{N}_1$ (shown with green arrow), which occurs in the "tooth" 1 (point D1 of the terminal phalanx). From the condition of equilibrium of the moments of forces $\sum M_{Ai} = 0$ we get: $N_1 h_1^A - S_1 h_2^A = 0$ or $N_1 = \frac{S_1 h_2^A}{h_1^A}$.

Here h_1^A - shoulder of the moment of effort $\bar{N}_1$ with respect to point A, h_2^A- shoulder of the moment of effort $\bar{S}_1$ (S_1 - the external force from the flexible traction element -1 is indicated by the green arrow). Moreover, $h_1^A = R_2 \sin(\frac{\alpha}{2})$, $h_2^A = R_2 - (R_1 + a)\cos(\frac{\alpha}{2})$. Let's find the internal effort $\bar{N}_2$ (shown with green arrow), which occurs in the tooth 2 (point D_2). Let's consider the equilibrium condition for the

moments of forces $\sum M_{Bi} = 0$. From the flexible connection fixed at the point E, at the point F there are two reactions, equal in magnitude S_1. They are directed: one from F to E, the second from F to K (shown by orange arrows). Their sum is $S_F = 2S_1 \sin(\frac{\alpha}{2})$ and it is directed from point F to point O. It creates a moment that presses the phalanx 2 to the fuel element. From the condition of equilibrium we have:

$$N_2 h_3^B - S_2 h_4^B + S_1 h_6^B + N_1 h_5^B - S_F h_3^B = 0 \quad (4)$$

Here $\dot{S}_2$ the external force from the flexible traction element-2 (shown by the green arrow) $h_3^B = h_1^A, h_4^B = h_2^A$, h_5^B - shoulder of the moment of effort $\dot{N}_1$, $h_5^B = R_2 \sin(3\frac{\alpha}{2})$. Let's find h_6^B - shoulder of the moment of effort $\dot{S}_1$ with respect to point B. The OB line in the XOY coordinate system: $X = 0$. Let's find the point E: $X_F = (R_1 + a)\cos(3\frac{\alpha}{2})$ $Y_F = (R_1 + a)\sin(3\frac{\alpha}{2})$. Let's find the point F: $X_F = (R_1 + a)\cos(3\frac{\alpha}{2})$ $Y_F = (R_1 + a)\sin(3\frac{\alpha}{2})$. Let's find the point C: $X_C = 0, Y_C = Y_E - \frac{X_E(Y_F - Y_E)}{X_F - X_E}$. $\angle OCE = 180^0 - 90^0 - 2\frac{\alpha}{2} = 45^0$. Length $BC = Y_C - R_2$, then . Efforts $\dot{N}_2$ is equal:

$$N_2 = \frac{1}{h_3^B}(S_2 h_4^B - S_1 h_6^B - N_1 h_5^B + S_F h_3^B) \quad (5)$$

Here some conditions arise. Efforts N_2 should be no less than or equal to the force in the tooth 1, that is $N_2 \geq N_1$. In order for the tooth 2 to exert no less force on the fuel element. Let's find the internal effort $\bar{N}_3$, which occurs in the tooth 3 (point D_3). We consider the equilibrium condition for the moments of forces $\sum M_{Gi} = 0$. From the flexible connection fixed at the point E, at the point F there are two reactions, equal in magnitude S_1. They are directed: one from K to F, the second from K to L. (shown by orange arrows). Their sum is $S_F = 2S_1 \sin(\frac{\alpha}{2})$ and it is directed from point K to point O. From the flexible connection fixed at the point E, at the point K there are two reactions, equal in magnitude S_1. They are directed: one from K to F, the second from K to L. (shown by orange arrows). Their sum is $S_{E1} = 2S_1 \sin(\frac{\alpha}{2})$ and it is directed from point K to point O. From the flexible connection fixed at the point F, at the point K there are two reactions, equal in magnitude S_2 and directed - one from K to F, the second from K to L. Their sum, which is equal to $S_{K2} = 2S_2 \sin(\frac{\alpha}{2})$ and it is directed from point K to point O. It creates a moment that presses the phalanx 1 against the fuel element. From the condition of equilibrium we obtain:

$$N_3 h_7^G - S_3 h_8^G + S_1 h_{10}^G + N_1 h_9^G + S_2 h_{12}^G + N_2 h_{11}^G - S_{K1} h_7^G - S_{K2} h_7^G = 0 \quad (6)$$

Where $\dot{S}_3$ external force from the flexible traction element-3 (shown by a green arrow), $h_7^G = h_3^B = h_1^A$, $h_{12}^G = h_6^B$, $h_8^G = h_4^B = h_2^A$, $h_{11}^G = h_9^G = h_5^B = R_2 \sin(3\alpha / 2)$. Let's find h_{10}^G as the shortest distance from the point G to the line passing through the points E and F in the coordinate system XOY. $X_G = -R_2 \sin(2\frac{\alpha}{2}), Y_G = R_2 \cos(2\frac{\alpha}{2})$ The equation of the line passing through points E and F: $\frac{X - X_E}{X_F - X_E} = \frac{Y - Y_E}{Y_F - Y_E}$ or $A_0 X + B_0 Y + C_0 = 0$ where the coefficients of this equation are $A_0 = Y_F - Y_E$, $B_0 = X_F - X_E$, $C_0 = (X_F - X_E)Y_E - (Y_F - Y_E)X_E$. Then, $h_{10}^G = \left| \frac{A_0 X_G + B_0 Y_G + C_0}{\sqrt{A_0^2 + B_0^2}} \right|$. Then condition of $\dot{N}_3$

$$N_3 = \frac{1}{h_7^G}(S_3 h_8^G - S_1 h_{10}^G - N_1 h_9^G - S_2 h_{12}^G - N_2 h_{11}^G + S_{K1} h_7^G + S_{K2} h_7^G) \quad (7)$$

Efforts N_3 should not be less than the forces in the teeth 1 and 2. In the tooth D_4, lying on the tile-base 0, from the condition of equilibrium of forces for the upper symmetrical part of the cross-section of the fuel element, we have: $-\bar{N}_1 - \bar{N}_2 - \bar{N}_3 - \bar{N}_4 = 0$ or $\bar{N}_4 = -\bar{N}_1 - \bar{N}_2 - \bar{N}_3$.

Corresponding values $\bar{N}_1', \bar{N}_2', \bar{N}_3', \bar{N}_4'$ in the symmetrical lower branch G'-B'-A'-M' at ponts D_1', D_2', D_3',grasp will be equal to them in magnitude and mirror-symmetrical in the direction of the axis OX. Have received a picture of static forces in a flat grasp model.

Now we are carrying out calculations, developed by us 3D models (Figure 7). The distribution of stresses, displacements, safety factors, deformations, contact pressures for various values of flexible traction forces simulated in six flexible connections and various metric parameters of the seizure is investigated. In general, when the optimal variants of both seizure schemes will obtained, then their comparative analysis would be carried out.

Conclusions

In this work, the problem of modeling two grasping schemes of the robot manipulator, developed by the authors, is considered in the case of overloading of solid highly radioactive waste of fuel elements. Two schemes, previously proposed by the authors as grasps, are investigated. One - rod, the second - innovative with flexible drives. For the grasps considered, some results are given: by

definition of the dependencies between the forces of the drive and the forces of gripping the part; static calculations for flat grasping models; 3D models are constructed; The strength and rigidity of the first 3D model is calculated. The work is carried out within the framework of the project AP05135609 "Institute of Mechanics and Engineering Science named after Academician UA Dzholdasbekov" of the Committee of the Ministry of Education and Science of the Republic of Kazakhstan.

Bibliography

1. Nofa Sh. "Handbook of Industrial Robotics". In: Mechanical engineering (1989): 480.
2. Kozirev UG. Industrial robots: a directory: Moscow: Mechanical Engineering, (1988): 392.
3. Kaiym T and Kaimov S. "The modeling of the theoretical and mathematical system and specifically the stochastic processes of the dynamical system an innovative mechanism for grasping of the robot for overloading the highly radioactive firm waste of fuel element from the secondary container into the main container". 2(422) News of The Academy of Sciences of the Republic of Kazakhstan, Almaty (2017): 412-417.
4. Kaiym T and Kaimov S. "Mathematical and Computer Modeling of Movement of The Executive Mechanism of the Adaptive Multipurpose Operating Part of Earth-moving and Construction Machine". Institute of Research and Journals IRAJ: The IRES 10th International conference, Czech Republic, c. Prague (2015): 196-199.
5. Y Zheng and WH Qian. "Limiting and Minimizing the Contact Forces in Multifingered Grasping". *Mechanism and Machine Theory* 41 (2006): 1247-1257.
6. Series of geology and engineering sciences (Proceedings of NAS RK): 2.422 (2017).
7. Digital Prototyping: Autodesk Inventor 2010 Official training course. - M.: DMK Press, (2010): 944.

Volume 3 Issue 6 June 2019
© All rights are reserved by Kaiym T.*, et al.*